

# Capturing non-local interaction effects in the Hubbard model: optimal mappings and limits of applicability

E. G. C. P. van Loon,<sup>1</sup> M. Schüler,<sup>2,3</sup> M. I. Katsnelson,<sup>1</sup> and T. O. Wehling<sup>2,3</sup>

<sup>1</sup>*Radboud University, Institute for Molecules and Materials,  
Heyendaalseweg 135, NL-6525 AJ Nijmegen, The Netherlands*

<sup>2</sup>*Universität Bremen, Institut für Theoretische Physik, Otto-Hahn-Allee 1, 28359 Bremen, Germany*

<sup>3</sup>*Universität Bremen, Bremen Center for Computational Materials Science, Am Fallturm 1, 28359 Bremen, Germany*

We investigate the Peierls-Feynman-Bogoliubov variational principle to map Hubbard models with nonlocal interactions to effective models with only local interactions. We study the renormalization of the local interaction induced by nearest-neighbor interaction and assess the quality of the effective Hubbard models in reproducing observables of the corresponding extended Hubbard models. We compare the renormalization of the local interactions as obtained from numerically exact determinant Quantum Monte Carlo to approximate but more generally applicable calculations using dual boson, dynamical mean field theory, and the random phase approximation. These more approximate approaches are crucial for any application with real materials in mind. Furthermore, we use the dual boson method to calculate observables of the extended Hubbard models directly and benchmark these against determinant Quantum Monte Carlo simulations of the effective Hubbard model.

## I. INTRODUCTION

Strongly correlated materials form one of the most challenging problems in condensed matter physics. Determining the electronic structure of a realistic material usually involves a multi-step process. First, the original problem is downfolded to a model system that describes the strongly correlated sector. Subsequently, an approximate solution for the model system is sought. The model system should be simple enough that is computationally tractable. The Hubbard model of itinerant electrons with a local interaction is a popular choice<sup>1-5</sup>. The original electrons of the model, however, have a long-range Coulomb interaction, so in general one would prefer to use an extended Hubbard model that also includes the non-local interactions, if this was computationally feasible.

The Peierls-Feynman-Bogoliubov variational principle<sup>6-8</sup> can be used to map extended Hubbard models with non-local interactions to effective models with only local interactions<sup>9</sup>. Previously, this method has been used to estimate the effective local interaction in materials with a hexagonal lattice, such as graphene<sup>9</sup>. Our focus here is on the square lattice Hubbard model with nearest-neighbor interaction. This system has been studied extensively as a testbed for theories developed over the last few years<sup>10-15</sup>. Of particular interest is how the renormalized effective interaction depends on the parameters of the Hubbard model. We show that the screening that leads to a renormalization of the local interaction depends strongly on interaction strength and filling.

We use four different computational methods, namely Determinant Quantum Monte Carlo<sup>16</sup> (DQMC), Dual Boson<sup>13,17,18</sup> (DB), Dynamical Mean-Field Theory<sup>19,20</sup> (DMFT) and the Random Phase Approximation (RPA). Two of these, DQMC and DMFT, are restricted to systems with local interaction. This is one of the main motivations for the effective Hubbard model approach:

the variational principle allows predictions about the extended Hubbard model using computational methods that are restricted to the Hubbard model. Since DQMC is numerically exact, it provides the perfect benchmark for the other methods. DMFT, on the other hand, is an approximation that can be extended to realistic, multi-orbital systems. Coupled with DFT, it forms the workhorse of the strongly correlated materials community. With the variational principle, non-local interactions can be incorporated into DMFT calculations with relative ease.

RPA and DB allow us to do calculations in the extended Hubbard model. The RPA has only a limited range of validity, since it is a theory for weakly interacting systems. At the same time, computationally it is the simplest of all the theories considered here. DB, on the other hand, is an extension of DMFT that incorporates strong correlation effects. We use it to determine observables in the presence of non-local interaction effects, and to study which observables follow the predictions of the variational principle.

The remainder of this work is structured as follows: In Sec. II we give a short overview of the variational principle used to determine the effective local interaction and of the methods used to obtain numerical results. In Sec. III, we determine the effective interaction strength in the half-filled Hubbard model. In Sec. IV, we use DQMC as benchmark for several observables calculated in DB, and in Sec. V we calculate these observables in the corresponding extended Hubbard model using DB. In Sec. VI and VII, we perform the same analysis for a strongly doped Hubbard model.

## II. METHODS

The extended Hubbard model on the square lattice with nearest-neighbor hopping reads

$$H = -t \sum_{\langle i,j \rangle, \sigma} c_{i\sigma}^\dagger c_{j\sigma} + U \sum_i n_{i\uparrow} n_{i\downarrow} + \frac{1}{2} \sum_{\substack{i \neq j \\ \sigma, \sigma'}} V_{ij} n_{i\sigma} n_{j\sigma'}, \quad (1)$$

where  $t$  is the nearest-neighbor hopping-matrix element and  $\langle i, j \rangle$  is a sum over nearest neighbors.  $U$  and  $V_{ij}$  are the local and non-local Coulomb matrix elements, respectively. The extended Hubbard model is a particular case of the so-called polar model that has been studied since the 1930's<sup>21–23</sup>.

We briefly review the main results of the variational method to map extended Hubbard models to *effective* Hubbard models with only local interactions<sup>9</sup>. The effective Hubbard model, reading

$$\tilde{H} = -t \sum_{\langle i,j \rangle, \sigma} c_{i\sigma}^\dagger c_{j\sigma} + \tilde{U} \sum_i n_{i\uparrow} n_{i\downarrow}, \quad (2)$$

is varied with respect to the effective local interaction  $\tilde{U}$  in order to minimize a free energy functional. This is equivalent to solving

$$\tilde{U} = U - \sum_{j \neq 0} V_{0j} \frac{\partial_{\tilde{U}} \langle n_0 n_j \rangle_{\tilde{H}}}{\partial_{\tilde{U}} \langle n_0 n_0 \rangle_{\tilde{H}}} \quad (3)$$

for  $\tilde{U}$ . For only nearest-neighbor interaction  $V$ , Eq. 3 simplifies to

$$\tilde{U} = U - V \alpha(\tilde{U}), \quad (4)$$

where we have introduced the nearest-neighbor renormalization strength

$$\alpha(\tilde{U}) = \sum_{\langle 0,j \rangle} \frac{\partial_{\tilde{U}} \langle n_0 n_j \rangle_{\tilde{H}}}{\partial_{\tilde{U}} \langle n_0 n_0 \rangle_{\tilde{H}}}. \quad (5)$$

Physically, this  $\alpha$  describes the effective screening of the local interaction by the non-local interaction effects.  $\alpha$  is a function of  $\tilde{U}$ , so it can be determined with knowledge of the effective local model alone.

The variational principle involves the calculation of charge correlation functions of the effective Hubbard model:  $\langle n_i n_j \rangle_{\tilde{H}}$ , where  $n_i = n_{i\uparrow} + n_{i\downarrow}$ . In this work, we use several methods to calculate the charge correlation functions: The determinant Monte Carlo method (DQMC<sup>16</sup>), the random phase approximation (RPA<sup>24</sup>), Dynamical Mean-Field Theory<sup>19,20</sup> and the dual boson method<sup>13,17</sup> (DB). In the remainder of this section, we give a short summary of these methods and associated numerical details. This part can safely be skipped on the first read.

The DQMC method is numerically exact and has been used for the variational principle before<sup>9</sup>. We use the

implementation of the QUEST code<sup>25</sup>. We obtain susceptibilities on Matsubara frequencies by Fourier transforming imaginary-time data. Disadvantages of DQMC are that it cannot be applied to the extended Hubbard model with non-local interaction straightforwardly<sup>26–28</sup> and that it suffers from a sign problem away from half-filled systems. We perform the DQMC calculations for finite  $12 \times 12$  (for half-filling) and  $8 \times 8$  (away from half-filling) systems with Trotter discretisation  $\Delta\tau = 0.025$ .

The RPA approach<sup>24</sup> is geared towards weakly-interacting systems. In a noninteracting system, the susceptibility is given by a ‘‘bubble’’ diagram of two Green’s functions,

$$\begin{aligned} \chi_0(i\omega_n, \mathbf{q}) &= -\frac{1}{\beta} \sum_{\nu_m} [G^0 G^0]_{\nu\omega\mathbf{q}}, \\ [G^0 G^0]_{\nu\omega\mathbf{q}} &= \frac{1}{N} \sum_{\mathbf{k}} G^0(i\nu_m + i\omega_n, \mathbf{k} + \mathbf{q}) G^0(\nu_m, \mathbf{k}), \end{aligned} \quad (6)$$

where  $G^0(\nu_m, \mathbf{k})$  is the noninteracting Green’s function,  $N$  is the number of  $\mathbf{k}$  points, and  $\nu_m, \omega_n$  are fermionic and bosonic Matsubara frequencies, respectively. Then, the susceptibility of the (weakly) interacting system is

$$\chi_{\text{RPA}}^{-1}(i\omega_n, \mathbf{q}) = \chi_0^{-1}(i\omega_n, \mathbf{q}) + U + V(\mathbf{q}), \quad (7)$$

Finally, the (equal-time) charge correlation functions are obtained by a Fourier transform to real space and by summing over the Matsubara frequency  $\omega_n$ :

$$\langle n_0 n_i \rangle - \langle n_0 \rangle \langle n_i \rangle = \frac{2}{\beta N} \sum_n \sum_{\mathbf{q}} e^{i\mathbf{q}\mathbf{r}_i} \chi_{\text{RPA}}(i\omega_n, \mathbf{q}). \quad (8)$$

Dynamical mean-field theory<sup>20</sup> is an approximate method that includes *local* correlation effects. The method applies to systems with local interactions only, i.e.,  $V = 0$ . The approach is based on a self-consistently determined auxiliary single-site problem. As in RPA, we obtain the correlation functions from the susceptibility in momentum and frequency space, which is given by

$$\chi_{\text{DMFT}}^{-1}(i\omega_n, \mathbf{q}) = -[\mathcal{G}\mathcal{G}](i\omega_n, \mathbf{q})^{-1} - \Gamma_{\omega_n}. \quad (9)$$

Here  $\mathcal{G}$  is the DMFT Green’s function, which has a local self-energy,  $\Gamma$  is the particle-hole irreducible two-particle vertex of the auxiliary single-site problem.  $[\mathcal{G}\mathcal{G}]$  is shorthand for the product of two Green’s functions. The equation has a matrix structure in fermionic frequencies<sup>20,29</sup>, which we have suppressed for notational convenience.

The dual boson method<sup>17</sup> is a diagrammatic extension of DMFT that allows for the treatment of non-local interactions directly, via an effective frequency dependent interaction  $U(\omega)$ . We apply self-consistent dual boson<sup>18</sup> in the charge and magnetic channel to obtain consistent correlation functions<sup>30</sup>. In dual boson, the expression for the susceptibility is

$$\chi_{\text{DB}}^{-1} = \chi_{\text{DMFT}}^{-1} + U + V(\mathbf{q}) - U(\omega), \quad (10)$$

with the important caveat that  $\chi_{\text{DMFT}}$  is determined using the DB auxiliary single-site problem, so that the  $\mathcal{G}$  and  $\Gamma$  that enter this equation are different from the ones in DMFT. DMFT is recovered when  $V(\mathbf{q}) = 0$  and  $U = U(\omega)$ .

The dual boson calculations are performed on a  $64 \times 64$  lattice. The dual boson implementation and the impurity solver are based on the ALPS libraries<sup>31</sup>. We use converged EDMFT calculations as the starting point for the DB self-consistency. The number of iterations needed to achieve the self-consistent hybridization and dynamic interaction increases from less than ten to approximately forty between  $U/t = 7$  and  $U/t = 8$ . This makes calculations at higher  $U$  very expensive computationally, and for that reason most of the DB calculations are at  $U/t < 8$ .

### III. EFFECTIVE LOCAL INTERACTION AT HALF-FILLING

Results from all methods presented in this work are obtained at the temperature  $\beta t = 2$ . We discuss the temperature dependence of our results at the end of this section. We use  $t = 1$  as the unit of energy.

To begin with, we discuss the half filled,  $\langle n_0 \rangle = 1.0$ , extended Hubbard model with only nearest-neighbor interaction terms. Therefore, the evaluation of Eq. 3 involves the calculation of the local and nearest-neighbor charge correlation functions. The results from DQMC, dual boson, DMFT and RPA are depicted in Fig. 1 for interaction strengths up to  $U/t = 10$ . As expected, all methods reproduce the non-interacting case exactly.

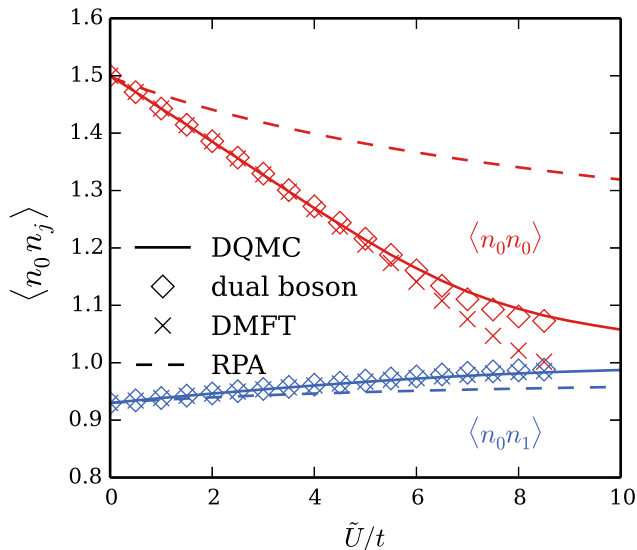


FIG. 1. (Color online) Local (red) and nearest-neighbor (blue) charge correlation functions of half filled nearest-neighbor hopping Hubbard model on a square lattice obtained from DQMC (full line), dual boson (crosses), DMFT (circles), and RPA (dashed line).

Wick's theorem theorem applies to the non-interacting system, so  $\langle n_0 n_0 \rangle = \langle n_0 \rangle + 2\langle n_{0\uparrow} \rangle \langle n_{0\downarrow} \rangle$  and  $\langle n_0 n_1 \rangle = \langle n_0 \rangle \langle n_1 \rangle - \sum_{\sigma} \langle c_{0\sigma}^{\dagger} c_{1\sigma} \rangle \langle c_{1\sigma}^{\dagger} c_{0\sigma} \rangle$ . The DQMC results approach the strong coupling result for  $U \gg t$ , where every site has one exactly electron and  $\langle n_0 n_0 \rangle = \langle n_0 \rangle = 1$  and  $\langle n_0 n_1 \rangle = \langle n_0 \rangle \langle n_1 \rangle = 1$ . For intermediate interaction strengths ( $U/t \lesssim 5$ ), results from DQMC, DMFT and dual boson are virtually indistinguishable on this scale. For larger interactions, differences between the exact DQMC and both the DMFT and the dual boson approximations are visible. Clearly, the dual boson method improves the DMFT results. The RPA results are considerably off the DQMC results at all nonzero interaction strengths. We note that the agreement between the methods is considerably better for the nearest-neighbor correlation function than for the local correlation function.

Next, we consider the nearest-neighbor renormalization strength  $\alpha(\tilde{U})$ , depicted in Fig. 2 (a), calculated from Eq. 5 with the different approximations. The simplest approximation to Eq. 3 discussed in Ref. 9 leads to  $\tilde{U} = U - V$ , i.e., a constant  $\alpha(\tilde{U}) = 1$ . This approximation can be derived by assuming that the correlation between sites that are not nearest neighbors is zero, i.e., that the system is very strongly localized.

The DQMC result indeed shows that the approximation  $\alpha(\tilde{U}) = 1$  is only valid for  $\tilde{U} \gg t$ . In this limit, sites that are more than one lattice spacing apart are uncorrelated, which is sufficient to prove  $\alpha = 1$ <sup>9</sup>. In fact,  $\alpha(\tilde{U})$  has a minimum at intermediate  $\tilde{U}$  before increasing towards 1. Dual boson agrees quite well with the exact DQMC results, with the largest deviations occurring around the minimum of  $\alpha$ . For  $\tilde{U}/t > 5$ , DMFT starts to deviate from DQMC. The DMFT results do show a minimum, however, that minimum is located at slightly larger  $\tilde{U}$ . For small interactions ( $\tilde{U}/t \lesssim 5$ ) the RPA result is off by  $\sim 15\%$  but qualitatively reproduces the behavior found in DQMC. However, RPA does not reproduce the noninteracting limit. The RPA result also misses the minimum found around  $U/t \sim 5$  and is off by a factor of 2 at large interactions.

To study the role of temperature, we have also done DQMC calculations at  $\beta t = 5$  instead of  $\beta t = 2$ . There,  $\alpha(\tilde{U})$  is qualitatively similar, as visible in Fig. 2(b). At  $\tilde{U} = 0$ , the nearest-neighbor renormalization strength  $\alpha$  is larger, as  $\tilde{U}$  increases it goes to a slightly deeper minimum that occurs at smaller  $\tilde{U}$ , and finally for large  $\tilde{U}$  the renormalization strength goes towards 1.

To give a sense of scale, we remind the reader that  $\beta t = 5$  and  $\tilde{U}/t = 4$  is close to the metal-insulator transition<sup>32</sup> and to the DMFT Néel temperature. The DMFT Mott metal-insulator transition, on the other hand, occurs at higher interaction strength  $\tilde{U}/t = 10 - 12$ .

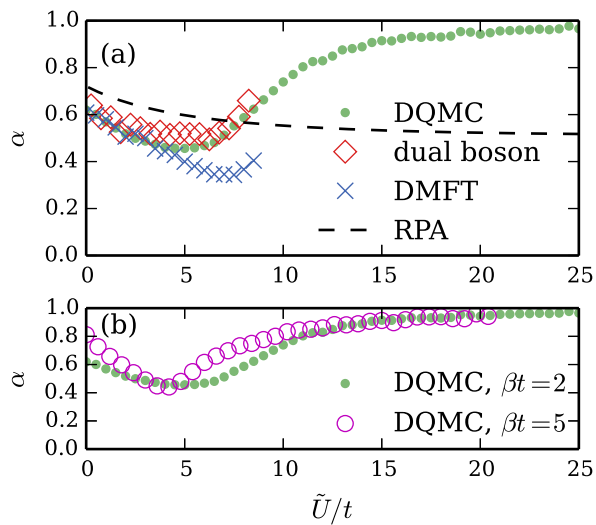


FIG. 2. (Color online) Nearest-neighbor renormalization strength  $\alpha(\tilde{U})$  of the half-filled nearest-neighbor hopping Hubbard model on a square lattice. (a)  $\alpha(\tilde{U})$  at  $\beta t = 2$ , as obtained from DQMC (green dots), dual boson (red diamonds), DMFT (blue crosses) and RPA (dashed line). (b) At  $\beta t = 2$  (green dots) and  $\beta t = 5$  (magenta circles) using DQMC.

#### IV. BENCHMARKING DUAL BOSON OBSERVABLES

The variational principle only deals with the free energy. In practical calculations, the main interest often lies with other observables, such as the Green's function and the double occupancy. The question is how well the optimal  $\tilde{U}$  Hubbard model reproduces the observables of the original extended Hubbard model with parameters  $U$  and  $V$ . We want to use dual boson to calculate the observables of the extended Hubbard model. Before we do that, we study the accuracy of dual boson at  $V = 0$ , where we can use DQMC as a benchmark.

In the previous section, we have seen that the DB results for the local and nearest-neighbor correlation function are accurate. In Fig. 3, we extend this conclusion to other observables, by comparing them to the DQMC values. In Fig. 3(a), we show the imaginary part of the local Green's function at the lowest Matsubara frequency and the double occupancy. The latter is equal to  $\langle n_0 n_0 \rangle / 2 - 1/2$ , cf. Fig. 1. In Fig. 3(b), we show some zero (Matsubara) frequency spin susceptibilities. These provide insight into the response of the system to static external fields. They are natural observables for dual boson, since we calculate the entire momentum and frequency dependent susceptibility according to Eq. (10). In DQMC, the susceptibility is determined as a function of imaginary time and we obtain the static component by a Fourier transform. In the figure, we show the  $q = (\pi, \pi)$  (checkerboard),  $q = (0, 0)$  (uniform) and  $q$ -averaged (local) spin susceptibility. In Fig. 3(c), we do the same for

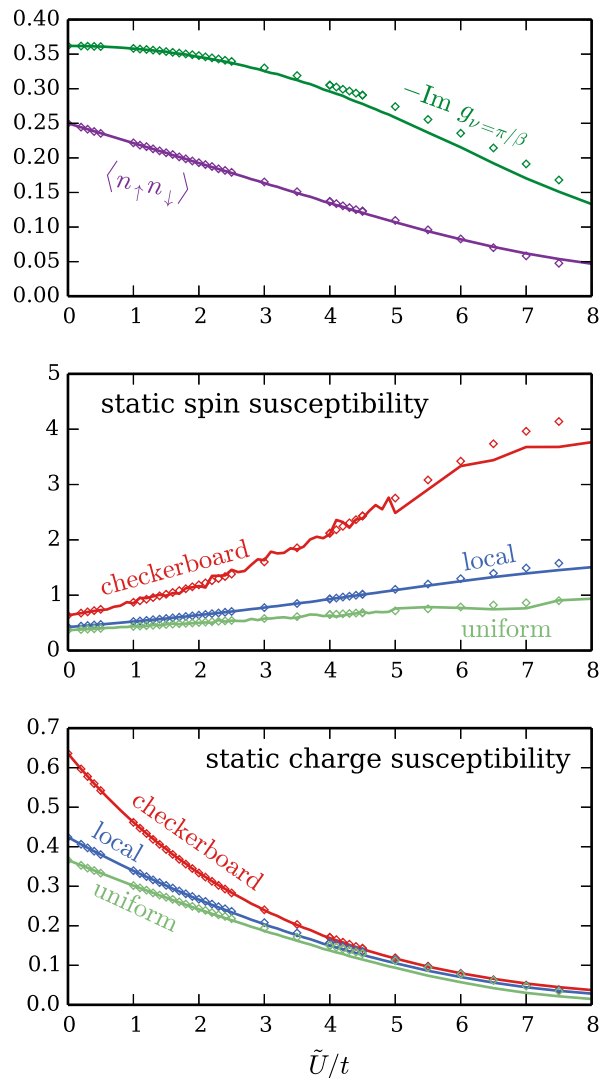


FIG. 3. Observables in the Hubbard model ( $V = 0$ ) obtained using DQMC (lines) and the dual boson method (diamonds).

the charge susceptibility. For all the observables shown, we find a good qualitative and quantitative agreement between DQMC and dual boson. Deviations start to set in at interaction strengths  $\tilde{U}/t \gtrsim 6$ .

Fig. 3 shows that the local repulsion  $\tilde{U}$  suppresses the double occupancy and charge excitations in general, whereas spin excitations are enhanced. The checkerboard spin susceptibility, corresponding to antiferromagnetism, increases the most. We should note that the temperature studied here,  $\beta t = 2$ , is above the Mott transition temperature, and all observables depend smoothly on  $\tilde{U}$ .

#### V. OBSERVABLES AT FINITE $V$

Now that we have confidence in the predictions of DB, we can use them as a benchmark for the variational principle at finite values of  $V$ . To study this,

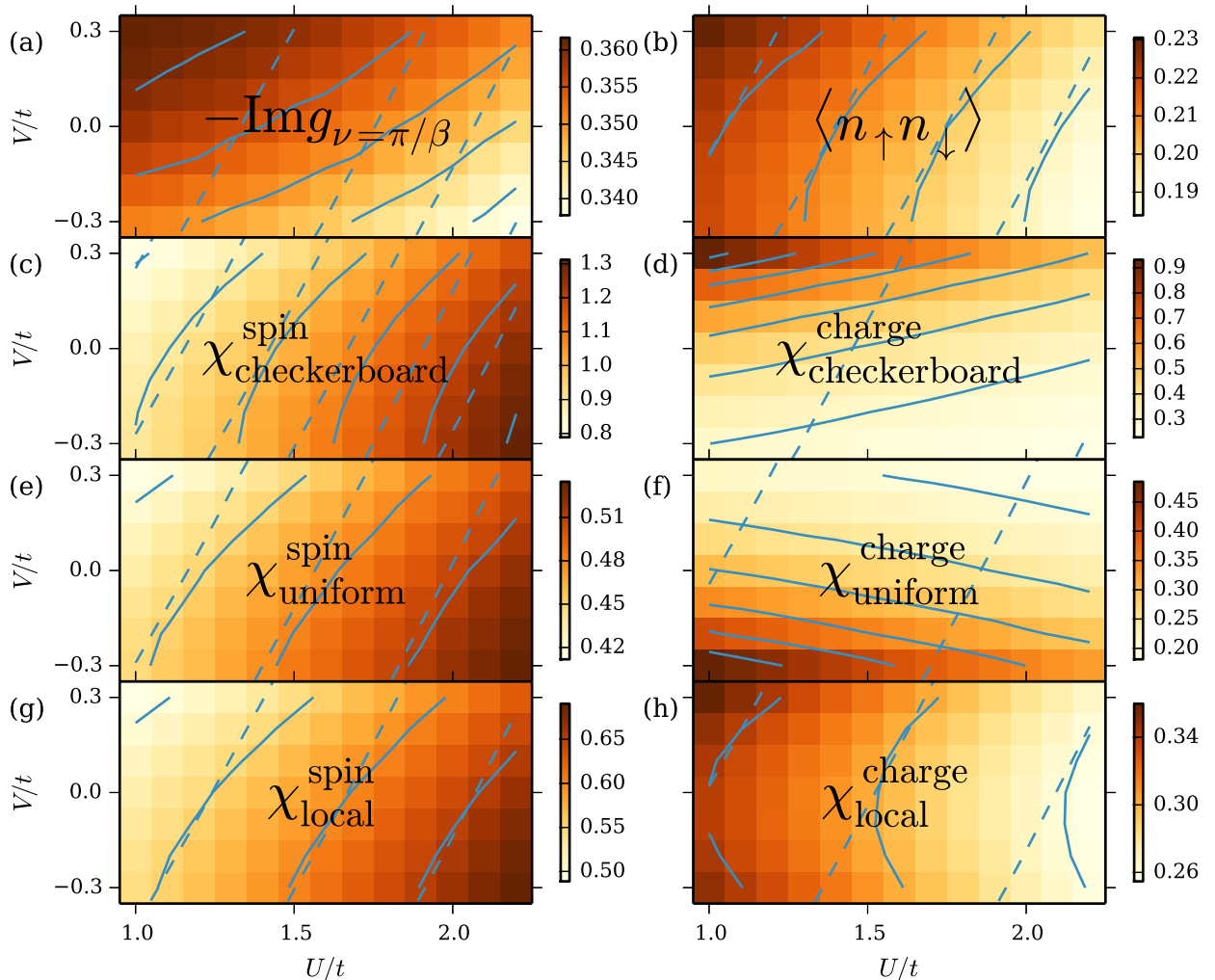


FIG. 4. Observables in the extended Hubbard model obtained using the dual boson method. Every colored square represents a dual boson calculation, they are separated by  $\Delta U = 0.1$  and  $\Delta V = 0.1$ . The solid lines show isolines where the observable is constant, the dashed lines show lines of constant  $\tilde{U}$  according to DQMC. The constant values of the isolines correspond to the tick labels in the colorbars.

we have done DB calculations for  $1.0 \leq U/t \leq 2.2$  and  $-0.3 \leq V/t \leq 0.3$ , the results of which are shown in Fig. 4. The colored plots give the value of the observable according to DB, with each colored square corresponding to a specific value of  $U$  and  $V$ . The solid lines are approximate isolines in the  $(U, V)$ -plane along which the observable is constant. The dashed lines, on the other hand, indicate constant  $\tilde{U}$ . If the variational principle were exact, these would be the isolines of the observables.

Fig. 4(a) contains the value of the Green's function on the first Matsubara frequency  $\pi/\beta$ ,  $-\text{Im} g_{\nu=\pi/\beta}$ . The DB observables does show a roughly linear dependence on  $V$ , albeit with a different slope than the variational principle predicts.

Next, in Fig. 4(b), for the double occupancy, there is a very good match between the dual boson calculations and the variational scheme. This correspondence is not accidental, the variational principle gives the exact double occupancy to first order in  $V$ , as is shown in Appendix A. The double occupancy is a special operator in this context, since it is directly connected to the variational parameter  $\tilde{U}$ . This explains the matching tangents at  $V = 0$  in Fig. 4(b). For larger  $|V|$ , the curvature in the DB results shows a divergence from the simple  $\tilde{U} = U - \alpha V$  prescription. As  $V$  becomes large compared to the Hubbard parameters  $\tilde{U}$  and  $t$ , it is no longer reasonable to expect the effective Hubbard model to do a good job in describing the relevant physics.

In Fig. 4(c), (e) and (g), we move to the zero-frequency spin susceptibilities, namely the checkerboard [ $q = (\pi, \pi)$ ], uniform [ $q = (0, 0)$ ] and local part [ $q$ -average] of the spin susceptibility, respectively. All three show a reasonable, though not perfect, match between the variational principle prediction and the dual boson results.

The corresponding correlation functions in the charge sector, in Fig. 4(d), (f) and (h), show a very different dependence on  $V$ . The checkerboard correlation function does have a linear dependence on  $V$ , with very small slope. In the uniform charge susceptibility, the sign of the  $V$ -dependence has changed, and for the local susceptibility the dependence is even quadratic instead of linear. This poor match is not a surprise. The non-local interaction  $V$  directly and explicitly enters the charge dynamics, as in Eq. (10), and the effective local interaction can only give a poor description of that dependence.

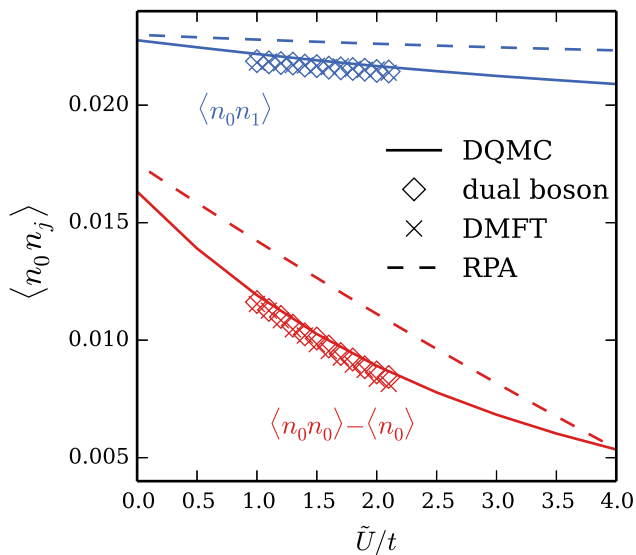


FIG. 5. (Color online) Local (red) and nearest-neighbor (blue) charge correlation functions of the hole doped ( $\langle n_0 \rangle = 0.18$ ) nearest-neighbor hopping Hubbard model on a square lattice obtained from DQMC (full line), dual boson (crosses), DMFT (circles), and RPA (dashed line).

## VI. EFFECTIVE LOCAL INTERACTION AWAY FROM HALF-FILLING

In order to study the performance of the different approximations as well as the renormalizations in dependence of the filling, we study the same Hubbard model as above with a filling of  $\langle n_0 \rangle = 0.18$ , well below the optimal filling for high- $T_c$  superconductors, of  $\langle n_0 \rangle \approx 0.8$ . At this small filling, the DQMC sign problem is not very severe and computations are feasible. In addition, we restrict ourselves to intermediate interaction strengths.

We follow the same approach as before and start by determining the charge correlation functions. These are

shown in Fig. 5. We come to very similar conclusions as in the case of half filling. DQMC, dual boson, and DMFT results agree closely in the investigated regime. RPA leads to correct trends but poor absolute agreement.

DQMC, DMFT and dual boson all operate in the grand-canonical ensemble, at fixed chemical potential  $\mu$ . The results at fixed density are obtained by interpolating between simulations at fixed chemical potential. This interpolation step introduces additional uncertainty into the determination of the correlators. This is especially visible when taking the numerical derivative of the correlation functions to obtain  $\alpha$ , as shown Fig. 6, since the difference quotient is very susceptible to noise.

Interestingly, for this hole doped case, the nearest-neighbor renormalization strength is negative, i.e., the nonlocal interaction increases the effective local interaction,  $\alpha < 0$ . This is in line with findings in the context of doped benzene models in Ref. 9 and can be understood in terms of Wigner crystallization<sup>33</sup>. In a very empty system, the local interaction  $\tilde{U}$  suppresses not only the probability to find a second electron on the same site, but also in the vicinity of the first electron. The effect of the non-local interaction  $V$  is also to keep electrons away from each other, so a positive  $V$  leads to a larger effective  $\tilde{U}$ . This renormalization increases for larger interaction. The DQMC, DMFT and dual boson result coincide within the (rather large) statistical uncertainty. While RPA gives the correct sign, it underestimates  $\alpha$  by a factor of two for small interactions and predicts a smaller renormalization for growing interaction, which is the wrong trend.

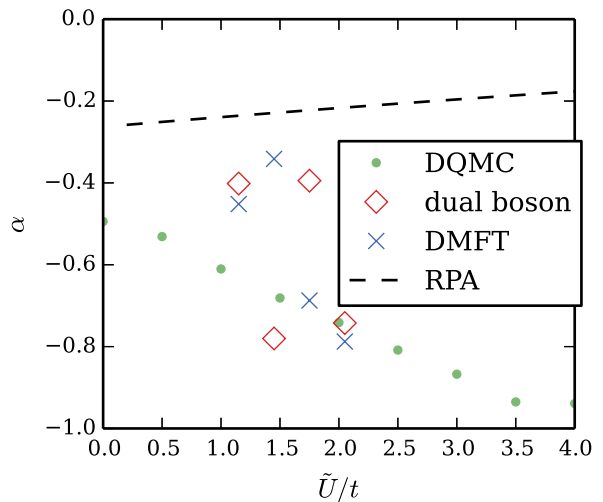


FIG. 6. (Color online) Nearest-neighbor interaction strength  $\alpha(\tilde{U})$  of the hole doped ( $\langle n_0 \rangle = 0.18$ ) nearest-neighbor hopping Hubbard model on a square lattice obtained from DQMC (green dots), dual boson (red diamonds), and RPA (dashed line).

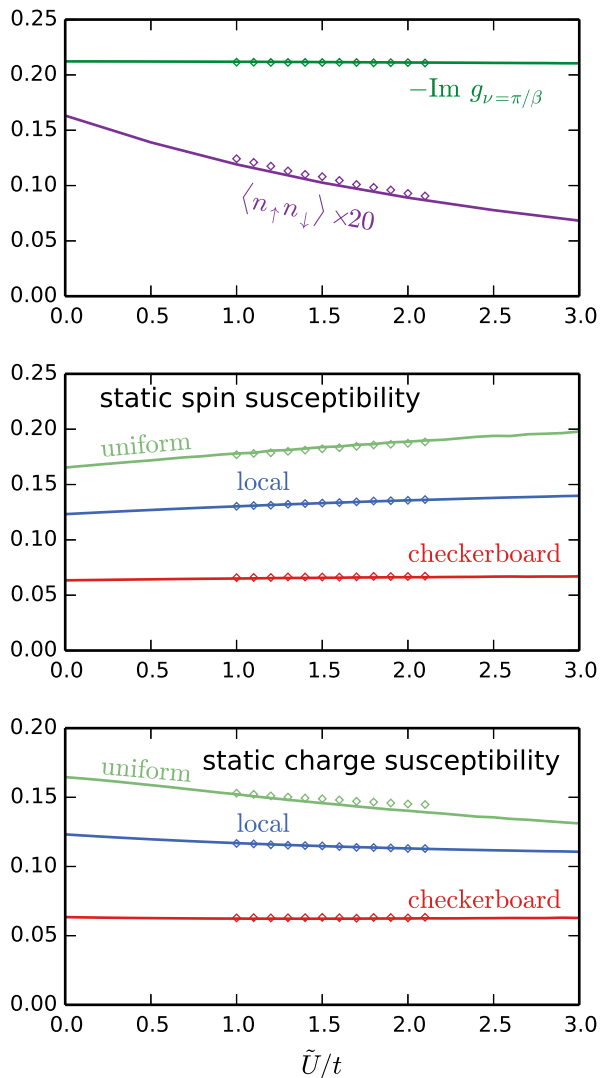


FIG. 7. Observables in the Hubbard model away from half-filling ( $\langle n_0 \rangle$  and  $V = 0$ ) obtained using DQMC (lines) and the dual boson method (diamonds), cf. Fig. 3 for the half-filled system.

## VII. OBSERVABLES IN DOPED SYSTEMS

Finally, we also study the observables of the doped system. As before, we start by comparing DQMC and DB observables at  $V = 0$ , this is shown in Fig. 7. We again find a good match between the DQMC and DB results. Secondly, we show the observables at finite  $V$  in Fig. 8. As before, the isolines predicted by DQMC are shown as dashed lines. Here, however, they do not match at all with the observables from dual boson.

Physically, the strongly doped  $\langle n_0 \rangle = 0.18$  system is very different from the half-filled Hubbard model. The local interaction  $U$  only affects electron pairs that occupy the same site, and as a result, an observable like  $g_{\nu=\pi/\beta}$  depends only very weakly on  $U$ , as seen in Fig. 7. As mentioned above, the local and non-local interaction

creates precursors to Wigner crystallization<sup>33</sup>. Even in the non-interacting system, the probability to find two electrons at the same site is  $\langle n_0 \rangle^2 / 4 < 1\%$ . As such, it is very difficult to encapsulate the effect of  $V$  into an effective  $\tilde{U}$ . Since the physics of the strongly-doped extended Hubbard model is not Hubbard-like, the effective mapping is not able to provide relevant results.

The susceptibility provides another clear difference between Figs. 4 and 8. In the half-filled model, perfect nesting of the Fermi surface with the checkerboard wavevector  $q = (\pi, \pi)$  creates a tendency towards checkerboard ordering (antiferromagnetic ordering in the spin channel) at lower temperatures. This is visible in the large values of the checkerboard susceptibilities in Fig. 4. At the much lower density  $\langle n_0 \rangle = 0.18$ , checkerboard ordering is not favored, and the checkerboard susceptibility is smaller than the uniform and local susceptibilities, and it depends only weakly on the interaction strength.

DMFT and DB both use a single-site auxiliary problem as the starting point of their approach. In this way, they are able to incorporate strong local correlation effects. Local correlation requires two particles at the same site, so this is expected to be less important at strong doping. Based on this, we can expect the non-local correlations that DB includes on top of DMFT to become more important at strong doping<sup>30,34</sup>, and we can also expect that the local correlation effects included in DB do not significantly improve on simpler theories like the GW-method.

This almost empty system clearly requires an explicit treatment of the nonlocal interactions. The extended Hubbard model is physically very different from the purely local Hubbard model, so any attempt to use the variational principle to relate the two is ill-fated.

## VIII. CONCLUSIONS AND DISCUSSION

We have studied the mapping of the extended Hubbard model onto effective local Hubbard models using a variational principle. In the half-filled Hubbard model, the simple prescription  $\tilde{U} = U - V$  is only applicable at very high values of  $U$ . At intermediate  $U$ , the effective renormalization of the local interaction  $\alpha$ , with  $\tilde{U} = U - \alpha V$ , is reduced by as much as a factor of 2.

To determine the effective interaction, the local and nearest-neighbor correlation function of the Hubbard model are needed. We find that the self-consistent dual boson approximation accurately reproduces the numerically exact DQMC results for the correlators, so that even the numerical derivatives come out similarly. DMFT performs qualitatively correct but quantitatively slightly worse at larger interaction strengths  $\tilde{U}/t > 5$ , and misses the location of the minimum of  $\alpha$ . RPA obtains the correct order of magnitude for the nearest-neighbor renormalization strength, however it is quantitatively off even at  $\tilde{U} = 0$ , does not have a minimum and fails in the limit of large interaction.

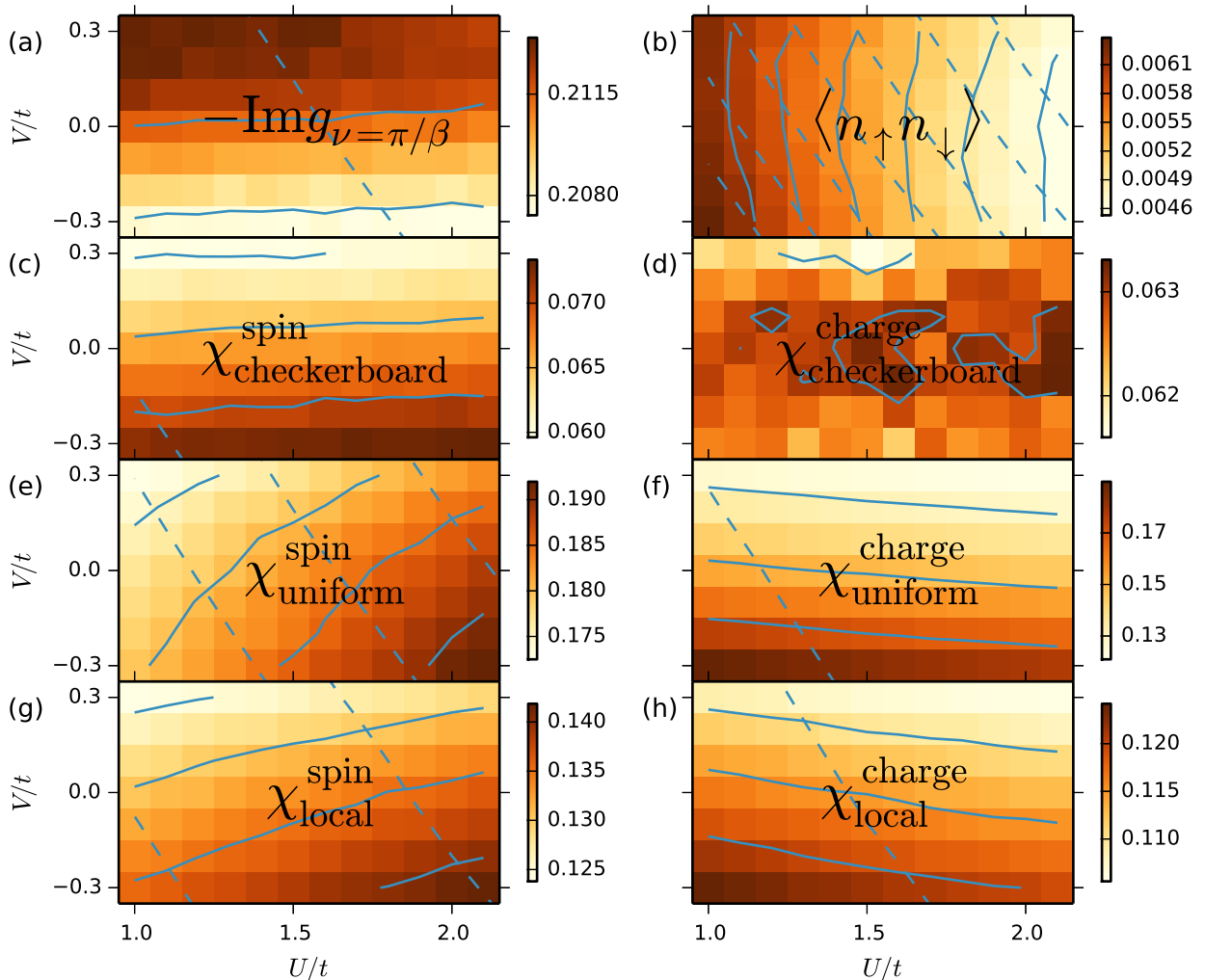


FIG. 8. Observables in the extended Hubbard model, away from half-filling at  $\langle n_0 \rangle = 0.18$ , obtained using the dual boson method. See Fig. 8 for the half-filled system.

For the nearly empty system (i.e. heavy hole doping,  $\langle n_0 \rangle = 0.18$ ), we find that non-local repulsion actually predicts a larger effective local interaction. Numerical calculations are more difficult in this parameter regime, which makes it difficult to assess exactly how well DMFT and DB match with the DQMC results.

We have also studied how observables of the extended Hubbard model behave as a function of  $V$ , again using the dual boson approach. The effective Hubbard model predictions work well for most observables at half-filling. For charge correlation functions, though, the effective Hubbard model does not match with the finite  $V$  results. This was to be expected, since the charge correlations depend explicitly on  $V$ .

Away from half-filling, the match between observables in DB and in the effective Hubbard model is much worse.

This parameter regime is dominated by Wigner crystallization physics, which is difficult to capture using the variational principle.

The contrasting behavior in these two scenarios teaches us that the mapping to an optimal local Hubbard model only has a chance to succeed when the physics of the system is essentially Hubbard-like. In the very empty system, where doubly occupied sites are rare, only changing the effective Hubbard parameter is insufficient to recover the Wigner localization physics. Similarly, the charge susceptibility in the half-filled system, which is directly driven by the non-local interaction, is not captured in the effective model. On the other hand, the extended Hubbard model at half-filling is sufficiently similar to the local Hubbard model that a renormalization of the interaction strength suffices to explain the Green's function, double

occupancy and spin susceptibility.

### ACKNOWLEDGMENTS

E.G.C.P. v. L. and M.I.K. acknowledge support from ERC Advanced Grant 338957 FEMTO/NANO. M.S. and T.O.W. acknowledge support from the Deutsche Forschungsgemeinschaft through the research unit 1346 and the University of Bremen through the Zentrale Forschungsförderung.

### Appendix A: Exact small- $V$ coefficient of the double occupancy

The Peierls-Feynman-Bogoliubov variational principle suggests to use an effective local interaction  $\tilde{U}$  to describe the effect of a nonlocal interaction  $V$ , with the prescription

$$\begin{aligned} \tilde{U} &= U - \alpha V, \\ \alpha &= - \sum_{j \text{ nn of } 0} \frac{\partial_{\tilde{U}} \langle n_0 n_j \rangle}{\partial_{\tilde{U}} \langle n_{0\uparrow} n_{0\downarrow} \rangle}, \end{aligned} \quad (\text{A1})$$

for that effective interaction, where we have restricted ourselves to nearest-neighbor interaction  $V$ .

For infinitesimally small nonlocal interaction  $V = dV$ , the change in effective local interaction  $U - \tilde{U} = \alpha dV = dU$  will also be small, and

$$\frac{dU}{dV} = \alpha. \quad (\text{A2})$$

The expression for  $\alpha$  contains two correlation functions, and both can be written as a derivative of the free

energy,

$$\sum_{j \text{ nn of } 0} \langle n_{0\uparrow} n_{j\sigma'} \rangle = - \partial_V F \quad (\text{A3})$$

$$\langle n_{0\uparrow} n_{0\downarrow} \rangle = - \partial_U F. \quad (\text{A4})$$

This allows us to write Equation (A1) in terms of second derivatives of the free energy. Assuming sufficient continuity of the free energy, the order of the partial derivatives can be changed,

$$\alpha = - \frac{\partial_V \partial_U F}{\partial_U \partial_U F}, \quad (\text{A5})$$

where we have replaced  $\partial_{\tilde{U}}$  by  $\partial_U$  since  $\tilde{U} - U$  is infinitesimal.

Now, we are interested in the value of the double occupancy, Equation (A4), as a function of  $U$  and  $V$ . Writing  $\langle n_{0\uparrow} n_{0\downarrow} \rangle = A(U, V) = -\partial_U F$ , we can expand around  $V = 0$ .

$$\begin{aligned} A(U, dV) &= A(U, 0) + dV \partial_V A \\ A(U - dU, 0) &= A(U, 0) + dU \partial_U A, \end{aligned} \quad (\text{A6})$$

so the optimal  $\tilde{U} = U - dU$  is given by

$$\begin{aligned} A(U, dV) &= A(U - dU, 0) \\ dV \partial_V A &= dU \partial_U A \\ \frac{dU}{dV} &= - \frac{\partial_V A}{\partial_U A} \\ &= - \frac{\partial_V \partial_U F}{\partial_U \partial_U F} \end{aligned} \quad (\text{A7})$$

This is exactly Equation (A5).

From this, we conclude that the Peierls-Feynman-Bogoliubov variational principle exactly reproduces the linear dependence on  $V$  of the double occupancy. The only required assumption is that the free energy is sufficiently smooth to allow the interchange of partial derivatives.

We stress that this proof only works for the double occupancy, not for other observables. The reason for this is that the double occupancy is exactly the observable obtained by deriving the free energy with respect to the variational parameter  $U$ .

<sup>1</sup> J. Hubbard, Proc. R. Soc. A. **276**, 238 (1963).

<sup>2</sup> M. C. Gutzwiller, Phys. Rev. Lett. **10**, 159 (1963).

<sup>3</sup> J. Kanamori, Prog. Theor. Phys. **30**, 275 (1963).

<sup>4</sup> J. Hubbard, Proc. R. Soc. A. **281**, 401 (1964).

<sup>5</sup> M. C. Gutzwiller, Phys. Rev. **134**, A923 (1964).

<sup>6</sup> R. Peierls, Phys. Rev. **54**, 918 (1938).

<sup>7</sup> N. N. Bogoliubov, Dokl. Akad. Nauk SSSR **119**, 244 (1958).

<sup>8</sup> R. P. Feynman, *Statistical Mechanics* (Benjamin, Reading Mass., 1972).

<sup>9</sup> M. Schüler, M. Rösner, T. O. Wehling, A. I. Lichtenstein, and M. I. Katsnelson, Physical Review Letters **111**, 036601 (2013).

<sup>10</sup> P. Sun and G. Kotliar, Phys. Rev. B **66**, 085120 (2002).

<sup>11</sup> T. Ayrál, S. Biermann, and P. Werner, Phys. Rev. B **87**, 125149 (2013).

<sup>12</sup> L. Huang, T. Ayrál, S. Biermann, and P. Werner, Phys. Rev. B **90**, 195114 (2014).

<sup>13</sup> E. G. C. P. van Loon, A. I. Lichtenstein, M. I. Katsnelson, O. Parcollet, and H. Hafermann, Physical Review B **90**,

- 235135 (2014).
- <sup>14</sup> G. Lhoutellier, R. Frésard, and A. M. Oleś, *Phys. Rev. B* **91**, 224410 (2015).
  - <sup>15</sup> R. Frésard, K. Steffen, and T. Kopp, *Journal of Physics: Conference Series* **702**, 012003 (2016).
  - <sup>16</sup> R. Blankenbecler, D. J. Scalapino, and R. L. Sugar, *Physical Review D* **24**, 2278 (1981).
  - <sup>17</sup> A. N. Rubtsov, M. I. Katsnelson, and A. I. Lichtenstein, *Annals of Physics* **327**, 1320 (2012).
  - <sup>18</sup> E. A. Stepanov, E. G. C. P. van Loon, A. A. Katanin, A. I. Lichtenstein, M. I. Katsnelson, and A. N. Rubtsov, *Phys. Rev. B* **93**, 045107 (2016).
  - <sup>19</sup> W. Metzner and D. Vollhardt, *Phys. Rev. Lett.* **62**, 324 (1989).
  - <sup>20</sup> A. Georges, G. Kotliar, W. Krauth, and M. J. Rozenberg, *Rev. Mod. Phys.* **68**, 13 (1996).
  - <sup>21</sup> S. Schubin and S. Wonsowsky, *Proceedings of the Royal Society of London Series A* **145**, 159 (1934).
  - <sup>22</sup> S. V. Vonsovsky and M. I. Katsnelson, *Journal of Physics C: Solid State Physics* **12**, 2043 (1979).
  - <sup>23</sup> S. V. Vonsovsky and M. I. Katsnelson, *Journal of Physics C: Solid State Physics* **12**, 2055 (1979).
  - <sup>24</sup> G. D. Mahan, *Many-Particle Physics*, *Physics of Solids and Liquids* (Plenum, 2000) 3rd ed.
  - <sup>25</sup> “QUantum Electron Simulation Toolbox” QUEST 1.3.0 A. Tomas, C-C. Chang, Z-J. Bai, and R. Scalettar, (<http://quest.ucdavis.edu/>).
  - <sup>26</sup> Y. Zhang and J. Callaway, *Phys. Rev. B* **39**, 9397 (1989).
  - <sup>27</sup> G. Dopf, A. Muramatsu, and W. Hanke, *Phys. Rev. Lett.* **68**, 353 (1992).
  - <sup>28</sup> M. Golor and S. Wessel, *Physical Review B* **92**, 195154 (2015).
  - <sup>29</sup> E. Pavarini, E. Koch, D. Vollhardt, and A. Lichtenstein, eds., *DMFT at 25: Infinite Dimensions*, Modeling and Simulation, Vol. 4, Autumn School on Correlated Electrons, Jülich (Germany), 15 Sep 2014 - 19 Sep 2014 (Forschungszentrum Jülich Zentralbibliothek, Verlag, Jülich, 2014).
  - <sup>30</sup> E. G. C. P. van Loon, F. Krien, H. Hafermann, E. A. Stepanov, A. I. Lichtenstein, and M. I. Katsnelson, *Phys. Rev. B* **93**, 155162 (2016).
  - <sup>31</sup> B. Bauer, L. D. Carr, H. G. Evertz, A. Feiguin, J. Freire, S. Fuchs, L. Gamper, J. Gukelberger, E. Gull, S. Guertler, A. Hehn, R. Igarashi, S. V. Isakov, D. Koop, P. N. Ma, P. Mates, H. Matsuo, O. Parcollet, G. Pawłowski, J. D. Picon, L. Pollet, E. Santos, V. W. Scarola, U. Schollwöck, C. Silva, B. Surer, S. Todo, S. Trebst, M. Troyer, M. L. Wall, P. Werner, and S. Wessel, *Journal of Statistical Mechanics: Theory and Experiment* **2011**, P05001 (2011).
  - <sup>32</sup> T. Schäfer, F. Geles, D. Rost, G. Rohringer, E. Arrigoni, K. Held, N. Blümer, M. Aichhorn, and A. Toschi, *Phys. Rev. B* **91**, 125109 (2015).
  - <sup>33</sup> E. Wigner, *Phys. Rev.* **46**, 1002 (1934).
  - <sup>34</sup> E. G. C. P. van Loon, H. Hafermann, A. I. Lichtenstein, and M. I. Katsnelson, *Phys. Rev. B* **92**, 085106 (2015).